Hydrogen Insertion Effects on the Electronic Structure of Equiatomic MgNi Traced by *ab initio* Calculations

Samir F. Matar[a,b], Adel F. Al Alam[c] and Naim Ouaini[c]

[a] CNRS, ICMCB, UPR 9048, F-33600 Pessac, France

[b] Université de Bordeaux, ICMCB, UPR 9048, F-33600 Pessac, France

[c] Université Saint Esprit de Kaslik (USEK), OCM (Optimisation et Charactérisation des Matériaux), URA GREVE, CSR-USEK, Jounieh, Lebanon

Reprint requests to S. F. Matar. E-mail: matar@icmcb-bordeaux.cnrs.fr

For equiatomic MgNi which can be hydrogenated up to the composition $MgNiH_{1.6}$ at an absorption/desorption temperature of 200 °C, the effects of hydrogen absorption are approached with the model structures $MgNiH$, $MgNiH_2$ and $MgNiH_3$. From full geometry optimization and calculated cohesive energies obtained within DFT, the $MgNiH_2$ composition close to the experimental limit is identified as most stable. Charge density analysis shows an increasingly covalent character of hydrogen: $MgNiH$ ($H^{-0.67}$) → $MgNiH_2$ ($H^{-0.63}$) → $MgNiH_3$ ($H^{-0.55}$). While Mg–Ni bonding prevails in MgNi and hydrogenated model phases, extra itinerant low-energy Ni states appear when hydrogen is introduced signaling Ni–H bonding which prevails over Mg–H as evidenced from total energy calculations and chemical bonding analyses.

Key words: Hydrogen, Equiatomic MgNi, Iono-covalent Character, Bader Charge, Chemical Bonding

Introduction

In spite of the large hydrogen sorption capacity of magnesium (7.6 wt.-%), the strong metal-hydrogen bonding in ionic MgH_2 prevents its use, and other Mg-based compounds were studied as candidates for hydrogen storage. It has been found early on that introducing nickel leads to materials with reversible adsorption ability such as in Mg_2NiH_4 [1].

The Mg-Ni system comprises Mg_2Ni and $MgNi_2$, but no report on the equiatomic composition has been published [2]. Recently, Kamata *et al.* [3] obtained equiatomic MgNi under HP/HT (5 GPa/300 °C) conditions. The structure is the tetragonal CuTi type with a small distortion with respect to cubic CsCl. The equiatomic phase was readily hydrogenated into $MgNiH_{1.6}$ and found to absorb and desorb hydrogen reversibly at 200 °C [3]. This result characterizes it as a hydride with 1.9 wt.-% H capacity, smaller than that of Mg_2NiH_4 (∼ 3.6 wt.-% H). However, from earlier work on amorphous nano-structured Mg-Ni a higher H content of 2.2 wt.-% in the equiatomic region was reported, *i. e.* with the composition $MgNiH_{1.84}$, close to $MgNiH_2$ [4]. Yet this amount of maximum hydrogen uptake is the lowest among nickel-based binary equiatomics such as YNi which can absorb up to 4 H per formula unit (FU) [5].

In the context of our continuing investigations of candidate compositions for hydrogen storage, focusing on the electronic structure of hydrogenated nickel-based intermetallics (*cf.* refs. [5, 6] and work cited therein), we address the bonding properties in the equiatomic MgNi and its hydrogenated compounds based on computations within the well-established quantum-theoretical density functional (DFT) framework [7, 8].

Computation Methods

Two computational methods within the DFT were used in a complementary manner. The Vienna *ab initio* simulation package (VASP) code [9, 10] allows geometry optimization and total energy calculations. For this we used the projector augmented wave (PAW)

method [10, 11], built within the generalized gradient approximation (GGA) scheme following Perdew, Burke and Ernzerhof (PBE) [12]. Also semi-core $2p$-Mg states were accounted for beside $3s$ valence states in the PAW potential construction. Preliminary calculations with local density approximation LDA [13] led to a largely underestimated volume *versus* the experiment. The conjugate-gradient algorithm [14] is used in this computational scheme to relax the atoms. The tetrahedron method with Blöchl corrections [11] as well as a Methfessel-Paxton [15] scheme were applied for both geometry relaxation and total energy calculations. Brillouin-zone (BZ) integrals were approximated using special k-point sampling. The optimization of the structural parameters was performed until the forces on the atoms were less than $0.02\,\mathrm{eV}\,\text{Å}^{-1}$ and all stress components less than $0.003\,\mathrm{eV}\,\text{Å}^{-3}$. The scalar relativistic calculations were converged at an energy cut-off of 400 eV for the plane-wave basis set with respect to the k-point integration with a starting mesh of $4 \times 4 \times 4$ up to $8 \times 8 \times 8$ for best convergence and relaxation to zero strains.

Then all-electron calculations with GGA were carried out for a full description of the electronic structure and the properties of chemical bonding, using the full potential scalar-relativistic augmented spherical wave (ASW) method [16, 17]. In the minimal ASW basis set, we chose the outermost shells to represent the valence states, and the matrix elements were constructed using partial waves up to $l_{\max} + 1 = 3$ for Mg and Ni, and $l_{\max} + 1 = 1$ for H. Self-consistency was achieved when charge transfers and energy changes between two successive cycles were below 10^{-8} and $10^{-6}\,\mathrm{eV}$, respectively. BZ integrations were performed using the linear tetrahedron method within the irreducible wedge. In order to optimize the basis set, additional augmented spherical waves were placed at carefully selected interstitial sites (IS). Besides the site projected density of states, we discuss qualitatively the pair interactions based on the overlap population analysis with the crystal orbital overlap population (COOP) [18]. In the plots, positive, negative, and zero COOP indicate bonding, anti-bonding, and non-bonding interactions, respectively.
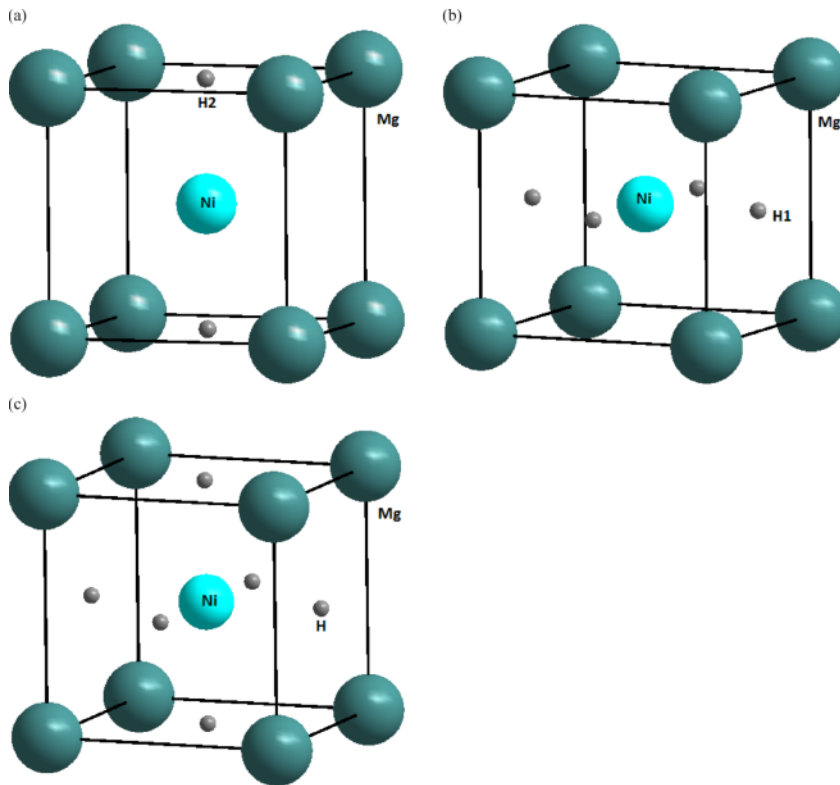

Fig. 1 (color online). MgNiH$_x$: the three model structures used in the calculations; a) MgNiH; b) MgNiH$_2$; c) MgNiH$_3$ (vertical: tetragonal axis c).

Geometry Optimization, Cohesive Energies and Charge Transfers

MgNi is found to crystallize in the tetragonal CuTi type with space group $P4/mmm$ and $a = 2.997$, $c = 3.166$ Å and $V = 28.44$ Å^3 per FU which can be considered as a tetragonally distorted CsCl cubic structure [3]. Upon hydrogenation the structure becomes cubic, $Pm\overline{3}m$ with $a = 3.215$ Å and $V = 33.23$ Å^3 per FU and a volume increase of $\Delta V/V \sim 17\%$.

Inserting hydrogen in the cubic structure leads to a random occupation of the threefold $3c$ positions within $Pm\overline{3}m$. However, this is difficult in computational modeling in which one can assume the occupation of only two out of the three $3c$ positions in order to approach the experimental stoichiometry MgNiH$_{1.6}$. Due to symmetry constraints the $3c$ positions split into ($1c$) $1/2$ $1/2$ 0 (model structure MgNiH with H2 in Table 1 and Fig. 1) and ($2e$) 0 $1/2$ $1/2$; $1/2$ 0 $1/2$ (MgNiH$_2$ with H1 in Table 1 and Fig. 1). The structure is then described within space group $P4/mmm$ (subgroup of $Pm\overline{3}m$). On the opposite, the full occupancy of the $3c$ sites such as in the MgNiH$_3$ model structure keeps the cubic symmetry. In order to appreciate the distortion effects and to follow the progressive hydrogen introduction, the model compositions Mg-

NiH, MgNiH$_2$ and MgNiH$_3$ besides MgNi have been examined. In the intermetallic CsCl-related structure the larger atom, *i. e.* Mg ($r = 1.60$ Å), is expected to be found at the origin (0 0 0), and the smaller one, *i. e.* Ni ($r = 1.24$ Å) at the body center ($1/2$ $1/2$ $1/2$) position. The two positions are equivalent as long as no neighbors are introduced, because the CsCl structure is composed of two interpenetrating simple cubic substructures. In fact the calculations with *straight* and *inverted* structures in both cubic and tetragonal MgNi led to identical volumes and energies. The results of the geometry optimization are given in Table 1, 2nd column; they show that the calculated volume of 28.32 Å^3 per FU is in the range of the experimental value ($V_{exp.} = 28.44$ Å^3 per FU). Close total energy magnitudes between the tetragonal and cubic structures are found, with the former identified as the ground state structure due to slightly lower energy, in agreement with experiment.

The introduction of hydrogen is modeled with the structures sketched in Fig. 1. They are characterized by Ni–H distances at $\sim a/2$ shorter than Mg–H at $\sim a\sqrt{2}/2$ and Mg–Ni at $\sim a\sqrt{3}/2$, considering a cube with an a edge for simplicity. Also from the positions of the hydrogen in the models MgNiH and MgNiH$_2$ the tetragonality ratios are expected as: $c/a > 1$ (elonga-

Symmetry		MgNi	MgNiH	MgNiH$_2$	MgNiH$_3$
$Pm\overline{3}m$	a, Å	3.05	–	–	3.32
(cubic)	V, Å^3	28.32			37.01
		(exp. 28.44)			
	$d_{\text{Mg-Ni}}$, Å	2.64	–	–	2.88
	$d_{\text{Ni-H1/H2}}$, Å				1.66
	$d_{\text{Mg-H1/H2}}$, Å	–			2.34
	Total energy per FU, eV	−7.45	–	–	−18.07 INV (−14.65)
	Cohesive energy per atom, eV	−0.435	–	–	−0.223
$P4/mmm$	a, Å	2.987	3.09	3.26	–
(tetragonal)	c/a	1.047	1.055	0.994	
	V, Å^3	28.30	31.08	34.4	
		(exp. 28.44)		(exp. 33.23)	
	$d_{\text{Mg-Ni}}$, Å	2.63	2.72	2.82	–
	$d_{\text{Ni-H1/H2}}$, Å		1.63	1.63	
	$d_{\text{Mg-H1/H2}}$, Å	–	2.18	2.30	
	Total energy per FU, eV	−7.46	−11.09 INV (−10.71)	−14.65 INV (−12.31)	–
	Cohesive energy per atom, eV	−0.437	−0.226	−0.247	–
Charge trends	$\Delta Q(\text{Mg})$	+1.61	+1.61	+1.66	+1.70
(in electrons)	$\Delta Q(\text{Ni})$	−1.61	−0.93	−0.41	−0.06
	$\Delta Q(\text{H1}) \times 2$	–	–	−0.63	−0.55
	$\Delta Q(\text{H2}) \times 1$	–	−0.67	–	−0.54

Table 1. Results of calculations for geometry optimizations and energy quantities of the studied model compounds.

tion) and $c/a < 1$ (flattening), respectively. The results shown in Table 1 confirm the trends for the distances ($d_{Mg-H} > d_{Ni-H}$) and the tetragonality c/a ratios close to 1, *i.e.* to a cubic structure. The volume increases following the series with additional inserted hydrogen atoms. $V_{calc.}(MgNiH_2) = 34.4$ Å^3 is slightly larger than the experimental value of 33.23 Å^3 due to 2 H instead of 1.6, but the agreement allows to assume a correct modeling of the experiment. In spite of starting with the assumption of a tetragonal structure with H1 and H2 at different hydrogen sites in model MgNiH$_3$, the calculations result in the cubic structure for the ground state which resembles the perovskite structure.

Nevertheless, for the sake of completeness, we further hypothesized the interchange of Mg and Ni positions in hydrogenated MgNi. This resulted in a substantial rise (destabilization) of the total energies, shown with 'INV' labels in Table 1, as a function of the amount of introduced hydrogen. The energy differences per atom in eV/FU units are then: $\Delta E(MgNiH) = 0.13$, $\Delta E(MgNiH_2) = 0.58$ and $\Delta E(MgNiH_3) = 0.79$, *i.e.* the higher the hydrogen content, the larger the destabilization. This confirms the stable configuration of the Mg (0 0 0) and Ni (1/2 1/2 1/2) positions with shorter Ni–H *versus* Mg–H distances, and the trend of hydrogen to bind with nickel preferentially.

The cohesive energies are obtained from energy differences between the total energy of the compound and those of the atomic constituents Mg and Ni and dihydrogen which have the following energies from PAW-GGA calculations (in eV): Mg (-1.543), Ni (-5.539) and H$_2$ (-6.577). The resulting cohesive energies in eV/atom are given in Table 1:

$$MgNi \ (-0.440) \rightarrow MgNiH \ (-0.226) \rightarrow$$
$$MgNiH_2 \ (-0.247) \rightarrow MgNiH_3 \ (-0.223)$$
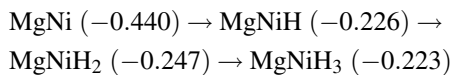
This trend can be interpreted as a destabilization of the intermetallic upon the introduction of hydrogen, but the least unstable composition is the one with 2 H. This resembles the experimental data where the observed MgNiH$_{1.6}$ composition [3] is the closest to our model MgNiH$_2$ which has the largest cohesive energy among the three model structures.

Focusing on MgNiH$_2$ the other twofold insertion sites $2f$ and $2g$ were examined for the sake of completeness. Full geometry optimization led respectively to total electronic energies: -12.22 and -11.62 eV

(with calculated $z = 0.605$), *i.e.* to less stable structures than MgNiH$_2$ with H at $2e$ positions (Table 1).

The analysis of the charge density issued from the self consistent calculations can be done using the AIM (atoms in molecules theory) approach [19] developed by Bader who devised an intuitive way of splitting molecules into atoms as based purely on the electronic charge density. Typically in chemical compounds, the charge density reaches a minimum between atoms, and this is a natural region to separate them from each other. Such an analysis can be useful when trends between similar compounds are examined; it does not constitute a tool for evaluating absolute ionizations. Bader's analysis is done using a fast algorithm operating on a charge density grid. The program [20] yields charge densities obtained from high precision VASP calculations and generates the total charge associated with each atom. The results of computed charge changes (ΔQ) are such that they lead to neutrality when the respective multiplicities are accounted for; the values are given for each atomic species in Table 1.

Due to the large electronegativity difference between Mg ($\chi = 1.31$) and Ni ($\chi = 1.91$), electron transfer is expected from Mg to Ni as observed for MgNi with a charge transfer of ± 1.61. In view of such large charge transfer featuring a partially ionic character, one should rather assume that s-like charges departing from Mg are close to free electron as in normal metals and delocalized over the whole MgNi crystal. The trends for the hydrides are such that in MgNiH the charge transfer is from Ni to H resulting in H$^{-0.67}$. This iono-covalent (in between -1, ionic, and $\sim < 0$, covalent) character of hydrogen is shifted to more covalent in MgNiH$_2$ with H$^{-0.63}$ and then to MgNiH$_3$ with H$^{-0.55}$. While in all three models the charge transfer is between Ni and H, the charge on Mg becomes slightly more ionic, changing from $+1.61$ to $+1.66$ and $+1.73$ along the series. At this point it becomes interesting to compare the relative charge results for cubic Mg$_2$NiH$_4$ on the one hand and rutile-type MgH$_2$ on the other hand calculated with the same conditions. In MgH$_2$ the obtained charges of ΔQ (Mg) $= +1.64$ and $\Delta Q(H) = -0.82$ show a much more ionic character, close to -1 for H. By contrast, Mg$_2$NiH$_4$ shows results closer to the presently studied model compounds: $\Delta Q(Mg) = +1.63$, $\Delta Q(Ni) = -0.71$ and $\Delta Q(H) = -0.64$. The charge carried by hydrogen is close to the one calculated for MgNiH$_2$. The covalent character brought into the electronic structure is

assigned mainly to nickel owing to its binding with hydrogen, as illustrated below.

Electronic Density of States and Chemical Bonding Properties

Starting from the calculated crystal structure data in Table 1, the electronic density of states and the chemical bonding were analyzed for the four studied compounds. At self consistent convergence, charge transfers follow the above discussed trends with small residues of ~ 0.15 electron into the interstitial spheres IS.

Fig. 2 shows in four panels the site projected density of states (PDOS) for tetragonal MgNi and the three

hydrogenated ternaries. Along the x axis the energy is with respect to the Fermi level E_{F}. As expected from the electronic configuration with Mg $(3s^2)$ as a main group metal and Ni $(4s^2 3d^8)$ as a transition metal, the valence band (VB) is dominated by Ni $3d$ states centered below E_{F} due to their large filling, Ni being at the end of the first transition metal period (Fig. 2a). Mg s states are distributed over the valence band with low intensity; this is also observed for hydrogen s states. The similar shapes of the respective PDOS signal a chemical bonding between the constituents. The character of the Ni PDOS changes along the four panels, becoming sharper – more localized – and showing extra structures in the hydrogenated compounds at the lower part
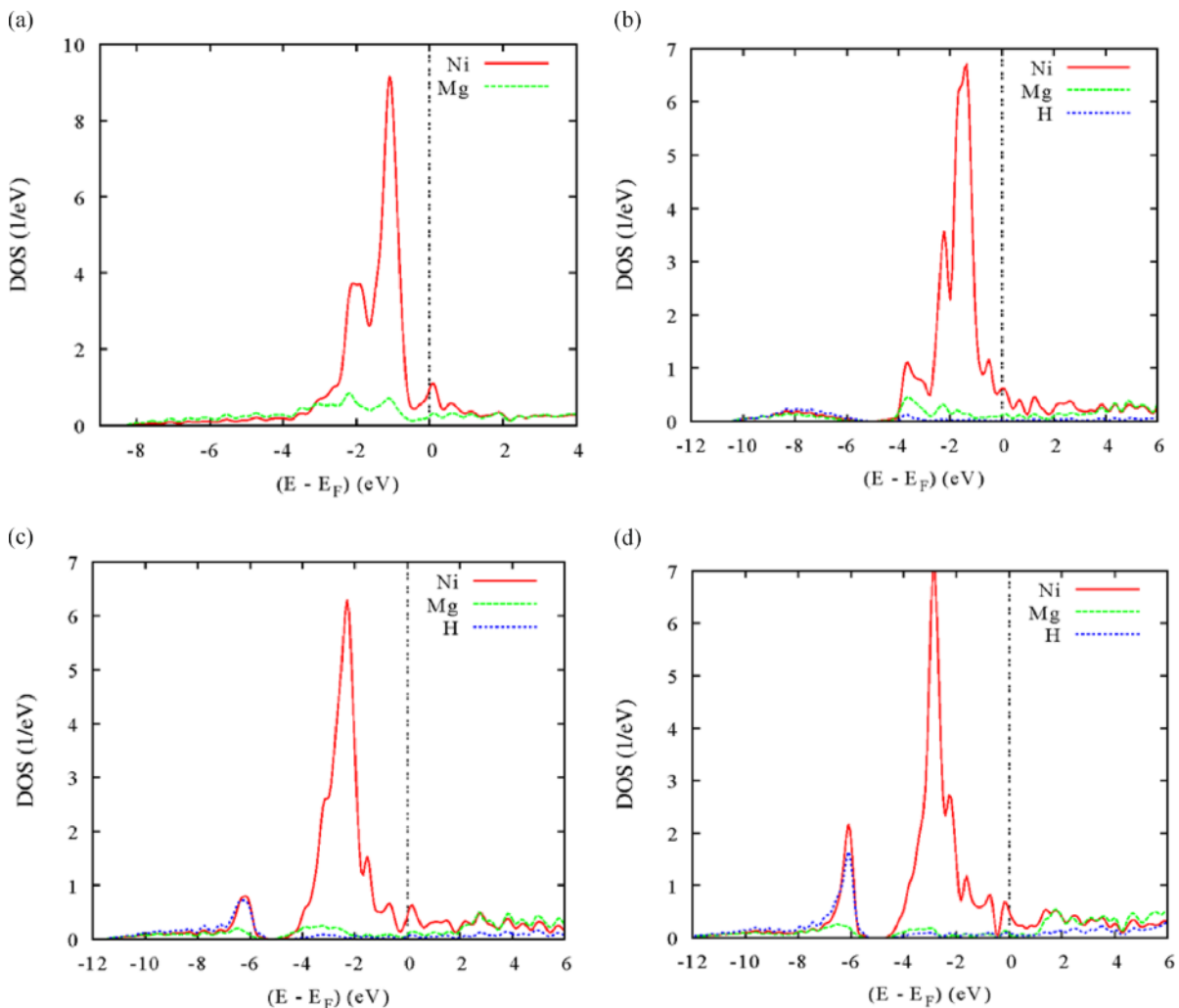

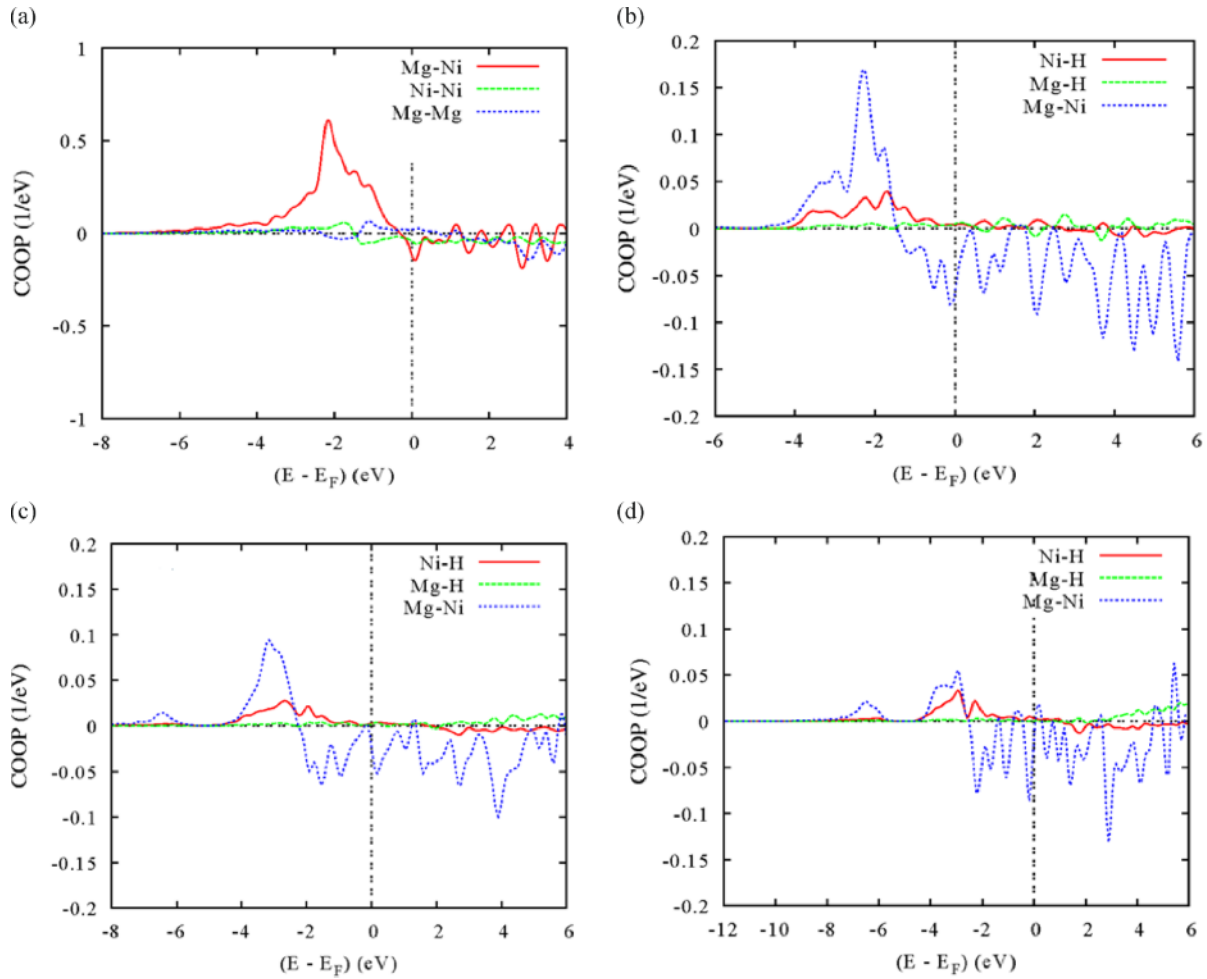Fig. 2 (color online). Site projected density of states: a) MgNi, b) MgNiH, c) MgNiH$_2$, and d) MgNiH$_3$.

(a)

(b)

(c)

(d)

Fig. 3 (color online). Chemical bonding for pair interactions (atom-to-atom) of a) MgNi, b) MgNiH, c) MgNiH$_2$, and d) MgNiH$_3$.

of the VB due to the quantum mixing with hydrogen states. This is illustrated in panels b)–d) of Fig. 2 with the same shape of the Ni and H PDOS in the energy window $\{-12, -6\,\text{eV}\}$ where itinerant states of Ni are found, and translates the chemical interaction between Ni and H as discussed below. The compounds are all metallic with no gap between the valence band (VB) and the conduction band (CB), and the Fermi level is crossing a low intensity DOS mainly from Ni with smaller contributions from Mg and H.

Fig. 3 shows the characteristics of chemical bonding with one atom of each kind for the sake of comparison. For MgNi in panel a), Mg–Ni bonding is dominant over Mg–Mg and Ni–Ni bonding. Antibonding Mg–

Ni COOP's are observed in the neighborhood of E_F and above. Then the structure is stabilized by Mg–Ni interactions which become anti-bonding in the neighborhood of E_F due to the already large filling of Ni d states. Upon hydrogen insertion – panels b) – d) – there are proportionally more electrons introduced, and E_F is pushed further up in energy leading to populated anti-bonding states. This likely arises from the involvement of more Ni electrons in the bonding with hydrogen, so that fewer electrons are available for Mg–Ni bonding; also the Mg–Ni distance increases (Table 1) leading to less overlap between the valence states of Mg and Ni. The consequence is the progressive destabilization of the metal substructure. Ni–H is the second

bonding intensity interaction with much higher intensity than Mg–H which is vanishingly small because of the larger Mg–H distance and because Mg–H bonds are non-directional as far as only *s*-like orbitals are involved.

Conclusion

For equiatomic MgNi, the effects of hydrogen uptake on the electronic structure and the iono-covalent character of bonding have been approached using model structures. Hydrogen insertion leads to a destabilization of the metal substructure through its binding with nickel. In agreement with experiments, the most stabilized hydrogenated model structure is $MgNiH_2$, close to the experimental composition ($MgNiH_{1.6}$) in which hydrogen is found to carry a charge of $H^{-0.65}$ with substantial covalent character. This is concomitant with a medium absorption/desorption temperature of $200\,^\circ$C whereas in ionic hydrides like MgH_2 the corresponding temperature is $\sim 350\,^\circ$C.

[1] J. J. Reilly, R. H. Wiswall, Jr., *Inorg. Chem.* **1968**, *7*, 2254.

[2] A. A. Nayeb-Hashemi, J. B. Clark, *Bull. Alloy Phase Diagram* **1985**, *6*, 238 – 244.

[3] Y. Kamata, T. Kuriiwa, A. Kamegawa, M. Okada, *Mater. Trans.* **2009**, *50*, 2064.

[4] S. Orimo, H. Fujii, K. Ikeda, Y. Fujikawa, Y. Kitano, *J. Alloys and Compd.* **1997**, *253 – 254*, 94.

[5] S. F. Matar, M. Nakhl, A. F. Al Alam, N. Ouaini, B. Chevalier, *Chem. Phys.* **2010**, *377*, 109.

[6] S. F. Matar, *Prog. Solid State Chem.* **2010**, *38*, 1.

[7] P. Hohenberg, W. Kohn, *Phys. Rev.* **1964**, *136 B*, 864.

[8] W. Kohn, L. J. Sham, *Phys. Rev.* **1965**, *140 A*, 1133.

[9] G. Kresse, J. Furthmüller, *Phys. Rev. B* **1996**, *54*, 11169.

[10] G. Kresse, J. Joubert, *Phys. Rev. B* **1999**, *59*, 1758.

[11] P. E. Blöchl, *Phys. Rev. B* **1994**, *50*, 17953.

[12] J. Perdew, K. Burke, M. Ernzerhof, *Phys. Rev. Lett.* **1996**, *77*, 3865.

[13] D. M. Ceperley, B. J. Alder, *Phys. Rev. Lett.* **1980**, *45*, 566.

[14] W. H. Press, B. P. Flannery, S. A. Teukolsky, W. T. Vetterling, *Numerical Recipes*, Cambridge University Press, New York **1986**.

[15] M. Methfessel, A. T. Paxton, *Phys. Rev. B* **1989**, *40*, 3616.

[16] A. R. Williams, J. Kübler, C. D. Gelatt, *Phys. Rev. B* **1979**, *19*, 6094.

[17] V. Eyert, *The Augmented Spherical Wave Method – A Comprehensive Treatment*, Lecture Notes in Physics, Springer, Heidelberg **2007**.

[18] R. Hoffmann, *Angew. Chem., Int. Ed. Engl.* **1987**, *26*, 846.

[19] R. Bader, *Chem. Rev.* **1991**, *91*, 893.

[20] W. Tang, E. Sanville, G. Henkelman, *J. Phys.: Condens. Matter* **2009**, *21*, 084204.